Virology 529 (2019) 205–215

Contents lists available at ScienceDirect

Virology

journal homepage: www.elsevier.com/locate/virology

The KSHV portal protein ORF43 is essential for the production of infectious viral particles

Daniela (Dana) Dünn-Kittenplon[a,b,c], Inna Kalt[a,c], Jean-Paul (Moshe) Lellouche[b,c], Ronit Sarid[a,c,*]

[a] The Mina and Everard Goodman Faculty of Life Sciences, Bar Ilan University, Ramat-Gan 5290002, Israel
[b] Department of Chemistry, Bar Ilan University, Ramat-Gan 5290002, Israel
[c] Advanced Materials and Nanotechnology Institute, Bar Ilan University, Ramat-Gan 5290002, Israel

ARTICLE INFO

Keywords:
Kaposi's sarcoma-associated herpesvirus, KSHV ORF43
Portal protein

ABSTRACT

Herpesvirus capsid assembly involves cleavage and packaging of the viral genome. The Kaposi's sarcoma-associated herpesvirus (KSHV) open reading frame 43 (*orf43*) encodes a putative portal protein. The portal complex functions as a gate through which DNA is packaged into the preformed procapsids, and is injected into the cell nucleus upon infection. The amino acid sequence of the portal proteins is conserved among herpesviruses. Here, we generated an antiserum to ORF43 and determined late expression kinetics of ORF43 along with its nuclear localization. We generated a recombinant KSHV mutant, which fails to express ORF43 (BAC16-ORF43-null). Assembled capsids were observed upon lytic induction of this virus; however, the released virions lacked viral DNA and thus could not establish infection. Ectopic expression of ORF43 rescued the ability to produce infectious particles. ORF43 antiserum and the recombinant ORF43-null virus can provide an experimental system for further studies of the portal functions and its interactions.

1. Introduction

Kaposi sarcoma-associated herpesvirus (KSHV), also known as human herpesvirus 8 (HHV-8), is one of eight known human herpesviruses. KSHV is a cancer-related gamma-2 herpesvirus which is etiologically implicated in all types of Kaposi's sarcoma (KS). In addition, KSHV is the causative agent of other disorders, including primary effusion lymphoma (PEL), multicentric Castleman's disease, and KSHV-inflammatory cytokine syndrome (Chang et al., 1994; Dittmer and Damania, 2013; Goncalves et al., 2017; Gramolelli and Schulz, 2015; Kalt et al., 2009; Mesri et al., 2010).

Like other herpesviruses, infectious KSHV virus particles are composed of a linear double-stranded DNA genome which is packed within a capsid that is coated with a proteinaceous tegument layer and an external phospholipid bilayer envelope spiked with viral glycoproteins (Heming et al., 2017). The KSHV capsid shares structural and morphological features with capsids of other herpesviruses, and its structural components are designated with reference to the herpes simplex virus types 1 (HSV-1) capsid (Trus et al., 2001). The capsid is approximately 125 nm in diameter with an icosahedral shell that consists of 955 copies of the major capsid protein (MCP) encoded by *orf25,* which forms 11 pentons and 150 hexons, comprising five and six MCP units, respectively (Wu et al., 2000). The pentons are located at 11 vertices of the icosahedral assembly while a 12-mer dodecameric cylindrical structure, formed by the portal protein, occupies a structurally unique 12th vertex (Chang et al., 2007; Trus et al., 2004). This ring-shaped structure forms a channel which functions as a gate for the cleavage, packaging and ejection of the viral genomic DNA. The MCP pentons and hexons are interconnected by 320 trimers, each composed of two ORF26 and one ORF62 molecules. The outer capsid shell is decorated with approximately 900 copies of the small capsid protein (SCP) encoded by *orf65*, which interacts with the MCP.

Assembly of the herpesvirus capsids is driven by interactions between the various capsid proteins. KSHV appears to share common features with the assembly mechanism of other herpesviruses (Baines, 2011; Brown and Newcomb, 2011; Deng et al., 2008; Heming et al., 2017). This process involves additional viral proteins that are commonly excluded from infectious viral particles, including the scaffold protein (SCAF) encoded by *orf17.5,* the protease protein encoded by *orf17,* and the tripartite terminase complex, which inserts and cleaves genomic viral DNA into the capsid through the portal, and is composed of proteins encoded by *orf7, orf29* and *orf67a.* Formation of capsids appears to be initiated by interactions of the portal complex with MCP, which pairs with the SCAF that then brings together additional MCP and SCAF molecules to ensure accurate curvature and capsid size. The idea that the portal ring serves as a nucleating center for pro-capsid

* Corresponding author at: The Mina and Everard Goodman Faculty of Life Sciences, Bar Ilan University, Ramat-Gan 5290002, Israel.
E-mail address: saridr@mail.biu.ac.il (R. Sarid).

https://doi.org/10.1016/j.virol.2019.01.028
Received 6 September 2018; Received in revised form 13 January 2019; Accepted 21 January 2019
Available online 01 February 2019
0042-6822/

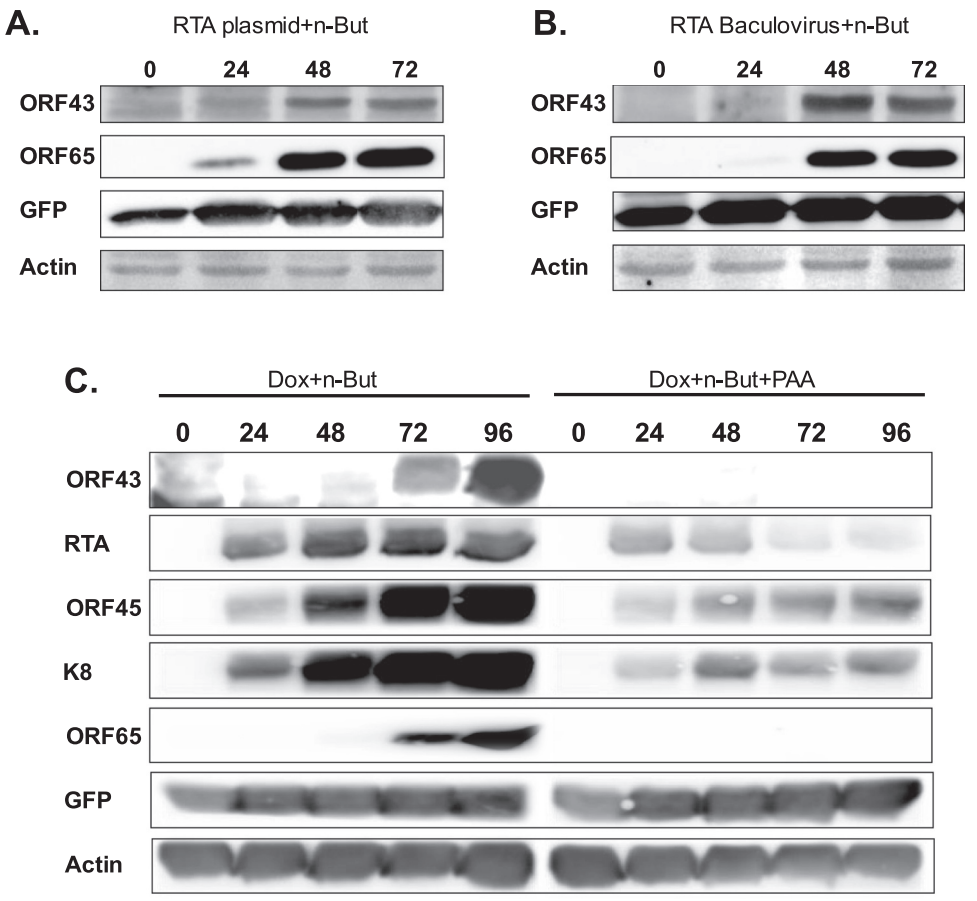

Fig. 1. *Expression kinetics of ORF43 protein following induction of lytic cycle.* HEK-293T-BAC16-infected cells were either transfected with RTA expression plasmid (A), or transduced with a recombinant baculovirus which expresses RTA under the control of CMV promoter (BacK50) (B), and treated with 1 mM sodium butyrate for 24, 48 and 72-hr. BAC16-infected iSLK cells were treated with 1 μg/ml Doxycycline (Dox) and 1 mM sodium butyrate with or with no phosphonoacetic acid (PAA) for 24, 48, 72 and 96-hr (C). Cells were lysed at the indicated time points, and 100 μg protein aliquots were analyzed by SDS-PAGE using anti-ORF43. Expression of the small capsid protein ORF65 was examined to confirm lytic induction (A and B), while expression of the immediate-early lytic gene products RTA and ORF45, the early lytic K-*b*-ZIP K8 protein and the late capsid protein ORF65 was examined to confirm inhibition of late gene expression by PAA (C). Expression of GFP was also examined. Actin was used as loading control.

assembly is supported by the observations of a single portal structure per capsid (Cardone et al., 2007; Chang et al., 2007; Deng et al., 2008; Motwani et al., 2017; Newcomb et al., 2005, 2003). Yet, *in-vitro* self-assembled capsids lacking the portal protein have been described (Newcomb et al., 2005; Perkins et al., 2008; Tatman et al., 1994; Thomsen et al., 1994), suggesting that the portal protein is not crucial for capsid assembly, and that capsids lacking the portal ring could potentially be assembled during natural infection. Capsid assembly results in the formation of sphere-shaped porous procapsids composed of the MCP, an inner shell which includes more than 1000 SCAF (ORF17.5) units and about 100 protease (ORF17) molecules, and an outer shell composed of the trimer of ORF26 and ORF62 proteins. Maturation of the viral capsids involves packaging of the viral genome along with cleavage of the inner SCAF and protease proteins, which results in deconstruction of the scaffolding complex that evacuates the pro-capsid (Cardone et al., 2012; Deng et al., 2008). However, only a small fraction of the assembled capsids contains DNA. In fact, three distinct types of capsids are produced, denoted A, B, and C. C-capsids are potentially infectious and are filled with viral genomic DNA, but lack scaffolding complexes. A-capsids are empty, perhaps as a result of inefficient DNA retention or unscheduled evacuation of SCAF components, and B-capsids lack DNA but contain variable amounts of residual scaffolding structures in different configurations (Deng et al., 2008; Nealon et al., 2001; Tandon et al., 2015; Tatman et al., 1994).

The portal protein, KSHV ORF43, shares 41–70% amino acid sequence similarity and predicted secondary and tertiary structure with known portal proteins that were already functionally characterized (Kornfeind and Visalli, 2018; Visalli and Howard, 2014). These include the prototype portal protein UL6, encoded by HSV-1, which was widely studied (Newcomb et al., 2001; Patel et al., 1996), pORF54 encoded by VZV (Visalli et al., 2014), pUL104 encoded by hCMV (Dittmer and Bogner, 2006; Holzenburg et al., 2009) and BBRF1 encoded by EBV (Pavlova et al., 2013), which were previously shown to be essential for the production of infectious progeny viruses. No detailed crystallographic data describing herpesvirus portal structures, including the KSHV portal protein, exist. Of note, recent cryoEM images of UL6 based on subnanometer resolution 3D reconstruction identified a unique portal-vertex-associated tegument complex, which is probably involved in genomic DNA retention (McElwee et al., 2018). Evidence for the existence of a single portal complex in KSHV capsids was previously obtained by using cryoelectron tomography (Deng et al., 2008). Molecular evidence supporting the function of KSHV ORF43 has not been published to date.

In the present study, we generated a KSHV ORF43-specific antiserum which was used to detect expression and localization of ORF43 during infection. We show that ORF43 is nuclear when expressed in the absence of other KSHV proteins. We constructed a recombinant ORF43-null KSHV genome and demonstrate that this clone establishes latent infection but fails to produce infectious viral particles. This phenotype was restored, though at different efficiencies, by expression of several untagged and tagged ORF43 proteins.

2. Results

2.1. KSHV ORF43 is a late viral protein, which is localized in the nucleus

To characterize the expression kinetics and the cellular distribution of ORF43 during KSHV infection, we generated rabbit polyclonal antiserum against an *E.coli* expressed protein consisting of the carboxyl-terminal KSHV ORF43 (amino acids 306–605). This anti-serum detected a ~60-kDa untagged and myc-tagged ORF43 proteins that were ectopically expressed in cells; these proteins were not recognized by the corresponding pre-immune serum (data not shown). Anti-myc antibody detected the same band of myc-tagged-ORF43. The observed molecular

mass of ~60-kDa was slightly lower than expected (68-kDa) based on the 605 amino acid comprising ORF43.

We used the antiserum in western blot assay to determine the expression of ORF43 protein during lytic virus reactivation in HEK-293T and in iSLK cells which were infected with a BAC16 recombinant KSHV clone. Lytic infection was induced upon expression of the replication and transcription activator (RTA) protein combined with treatment with the histone deacetylase inhibitor, sodium butyrate. As shown in Fig. 1A and B, the expression level of ORF43 increased over time and shared a similar pattern with the small capsid protein ORF65, which is classified as late lytic protein. Similar pattern was observed in iSLK cells that were treated with Doxycycline and sodium butyrate to induce lytic reactivation. Furthermore, combined treatment with the viral DNA polymerase inhibitor phosphonoacetic acid (PAA), which inhibits expression of late viral genes, completely abolished the expression of ORF43. Similar results were obtained for the late lytic small capsid protein ORF65, whereas the expression of ORF45 and K-*b*-ZIP K8, representing immediate-early and early gene products, respectively, continued though at relatively lower levels. Similarly, RTA which is expressed in iSLK cells under the control of doxycycline, as well as an immediate-early lytic gene product, continued to be expressed. These findings support the classification of ORF43 as a late lytic protein (Fig. 1C).

To determine the subcellular localization of ORF43 protein during lytic reactivation, we used an immunofluorescence assay with ORF43 antiserum. Cells were co-stained with the small capsid protein ORF65 antibody to enable identification of cells undergoing lytic reactivation. As shown in Fig. 2, ORF43 co-localized with ORF65, and was predominantly expressed in the nucleus within typical viral assembly structures (Fig. 2). However, newly assembled virions could be detected by ORF65 antibody, whereas ORF43 antiserum failed to detect virions (Fig. 2). This might be due to the relatively low copies of ORF43 (12 protein units) within each viral particle as compared to the large copy number of ORF65 protein (~900 protein units), or due to lower sensitivity of the ORF43 antiserum. Alternatively, it is possible that the epitope/s which are recognized by ORF43 antibody, are hidden within the capsid structure, and therefore cannot be detected by our ORF43 antibody. This hypothesis is supported by cryoelectron tomography reconstructions which illustrated the KSHV portal vertex as an internal structure with respect to the capsid floor (Deng et al., 2007, 2008; Kornfeind and Visalli, 2018). Of note, immunofluorescence staining of ORF43 protein during *de novo* infection with recombinant BAC16-mCherry-ORF45 virions (Bergson et al., 2014), which incorporate mCherry-ORF45 in the tegument, detected ORF43 in a minor fraction of incoming virions, suggesting the occurrence of a rare virion conformation which enables access of the antibody to ORF43 (data not shown). In line with the cellular distribution of ORF43 during lytic reactivation, un-tagged and myc-tagged ORF43 proteins that were ectopically expressed in uninfected cells were predominantly nuclear, suggesting that nuclear targeting of ORF43 does not require viral protein expression (Fig. 3). However, the cellular distribution of ORF43 was largely affected by the addition of HA and mCherry tags, resulting in cytoplasmic localization of ORF43 protein, which also formed noticeable aggregates when fused to HA-tag (Fig. 3).

2.2. Construction of BAC16-ORF43-null recombinant viral clone

To construct a mutant virus that fails to express ORF43, we used the complete KSHV BAC16 clone, which enables genetic manipulation of the KSHV genome in *E. coli* using the two-step Red-mediated recombination approach (Brulois et al., 2012; Tischer et al., 2006). The N-terminal of ORF43 coding sequence overlaps the C-terminal coding sequence of ORF44, and it was not possible to generate an *orf43*-stop mutation right after its first methionine without affecting the overlapping reading frame. Therefore, we introduced two stop codons within a downstream sequence that does not overlap *orf44* gene (TCC

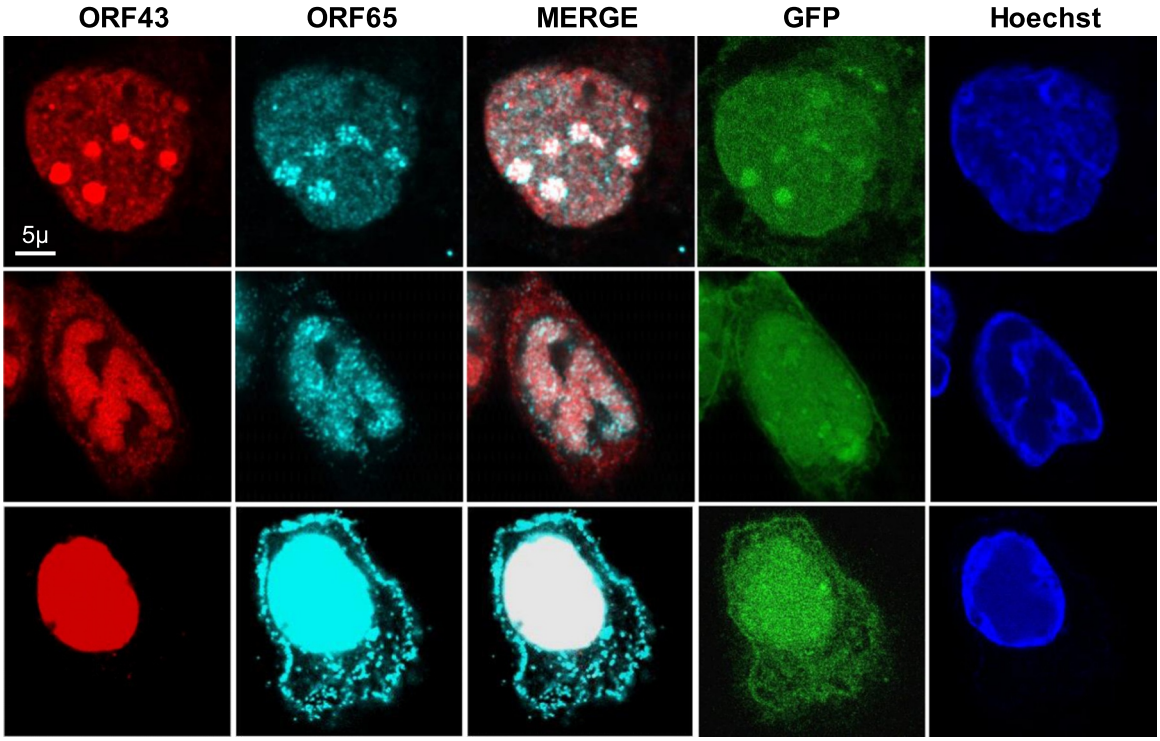

Fig. 2. *Cellular distribution of ORF43 in BAC16-infected iSLK cells undergoing lytic infection.* Latently BAC16-infected iSLK cells were treated with 1 μg/ml Doxycycline (Dox) and 1 mM sodium butyrate to induce lytic reactivation. Cells were fixed 72-hr post induction, and ORF43 was probed with rabbit anti-ORF43 serum followed by anti-rabbit Cy3-conjugated secondary antibody (red). Subsequently, the cells were probed with anti-ORF65 antibody and anti-mouse Alexa 647-conjugated secondary antibody (cyan). Images of the corresponding GFP expression, which indicates infection, and staining of nuclear DNA by Hoechst are also shown. Different cell localization patterns of ORF43 and ORF65 are presented to demonstrate different stages in the progression of the lytic cycle.

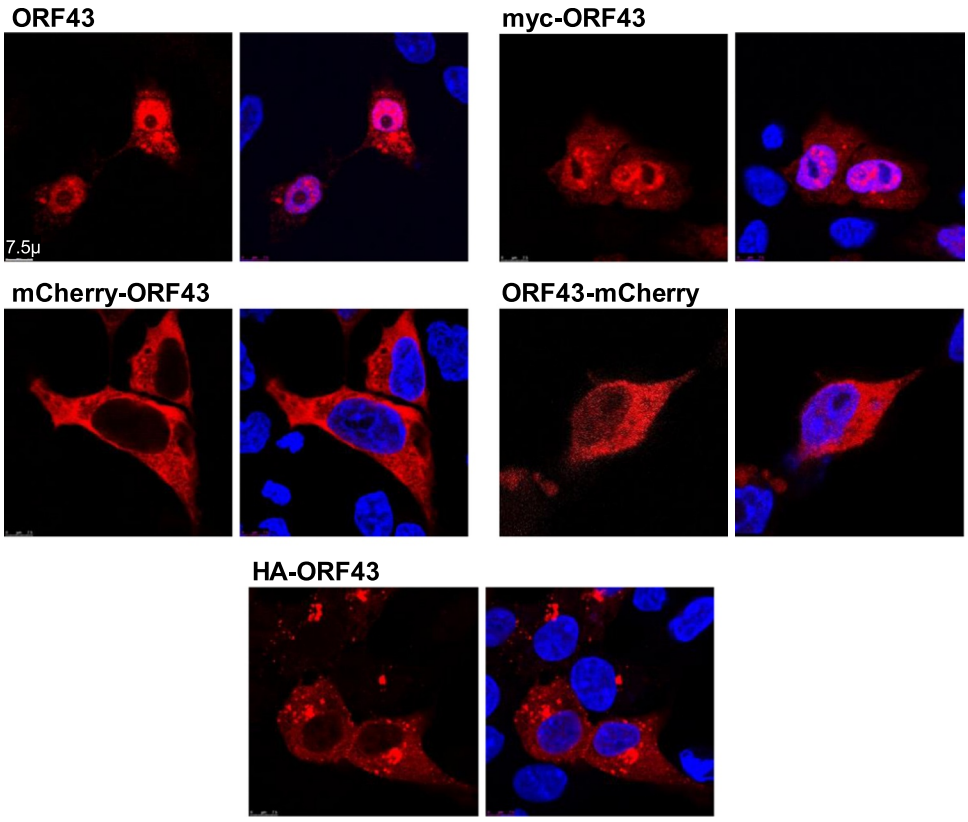

Fig. 3. *Cellular distribution of ectopically expressed ORF43 in uninfected cells.* HEK-293T cells were transfected with the indicated un-tagged or tagged ORF43 expression vectors and fixed after 28-hr. Cells were probed with anti-ORF43 serum followed by anti-rabbit Cy3-conjugated secondary antibody, or with myc or HA antibody followed by anti-mouse Rhodamine-conjugated secondary antibody. Cells that were transfected with mCherry-ORF43 expression vector were directly visualized. Nuclei were stained with Hoechst.

CTCTTT → TAGCTCTAG) (Fig. 4A). The resulting virus was expected to fail to express full-length ORF43 protein, but instead expresses a short 21-amino acid peptide. Restriction enzyme analysis with *Xba*I showed the insertion of a kanamycin-resistance cassette after the first recombination, and appropriate restriction pattern after the second recombination (Fig. 4B). The recombinant viral clone, designated BAC16-ORF43-null, was confirmed by diagnostic PCR and sequence analysis, thereby ensuring the mutations and appropriate junctions in the recombination domain (Fig. 4C).

2.3. BAC16-ORF43-null-infected cells do not produce infectious viruses

To determine whether ORF43 is required for the production of infectious viral particles, we transfected the recombinant BAC16-ORF43-null DNA into HEK-293T cells. As a positive control, we transfected wild-type (WT) BAC16 DNA. Transfected cells were selected with hygromycin and, as expected, constitutively expressed GFP under the control of the cellular EF1-α promoter (Brulois et al., 2012). We independently established three WT and three mutant HEK-293T cell lines containing BAC16-ORF43-null and BAC16 DNA, respectively. To examine whether BAC16-ORF43-null-infected cells can undergo lytic induction and produce infectious viruses, we transduced these cells with a recombinant baculovirus that expresses RTA (BacK50), and treated with sodium butyrate to induce lytic virus reactivation. As shown in Fig. 5, at 72-hr post induction WT BAC16-infected cells demonstrated expression of ORF65 and ORF43 whereas BAC16-ORF43-null-infected cells expressed ORF65 but failed to express ORF43. Furthermore, 96-hr following lytic induction, we collected supernatants, removed cell debris by centrifugation and filtration, and examined the presence of infectious particles following inoculation of naïve SLK or iSLK cells by spinoculation. As expected, GFP-positive cells were obtained following exposure of SLK cells to supernatants from WT BAC16-infected cells. In contrast, not a single GFP-positive cell was detected in SLK cells that were inoculated with supernatants from BAC16-ORF43-null-infected cells. This suggests that BAC16-ORF43-null-infected cells fail to produce infectious progeny viruses.

To enable the packaging of the mutated BAC16-ORF43-null genome, we transfected different ORF43 expression vectors 24-hr prior to lytic induction, and assayed the presence of infectious progeny viruses in supernatants that were collected 96-hr post induction. WB analysis with ORF65 antibodies confirmed lytic induction while ORF43 antisera confirmed expression of un-tagged and tagged ORF43 proteins (Fig. 6A). These experiments revealed that transfection of diverse ORF43 expression vectors, including un-tagged ORF43, N-terminal myc-tagged, N-terminal HA-tagged, and N- and C-terminal mCherry-tagged ORF43, enabled the production of infectious viral particles. Of note, we repeatedly observed relatively low levels of infectious viruses in supernatants from cells expressing mCherry-tagged ORF43, in particular C-terminal mCherry tag, while expression of untagged, myc or HA-tagged ORF43 enabled production of similar amounts of infectious particles (Fig. 6B). Using this approach, we established BAC16-ORF43-null-infected iSLK cells that expressed lytic proteins upon reactivation (Fig. 7A). To ensure that the infected iSLK cells carried a BAC16-ORF43-null genome rather than a WT BAC16 genome, we confirmed the desired mutations by sequence analysis of an amplified PCR product spanning this region. In addition, we designed two sets of PCR primers that selectively base-pair and amplify WT or mutated *orf43*. Using these sets, we obtained a PCR amplification product from WT BAC16-iSLK cells with the WT primer set, and not with the mutated *orf43* primer set. In contrast, a PCR amplification product was obtained only with mutated *orf43* primers when using DNA from iSLK cells that were infected with BAC16-ORF43-null virions, produced following ectopic expression of ORF43 with or with no tag (Fig. 7B). So far, we cannot rule out the occurrence of rare homologues recombination events between a segment of the ORF43 expression vector and the viral genome leading to the production of a small number of revertant genomes generating

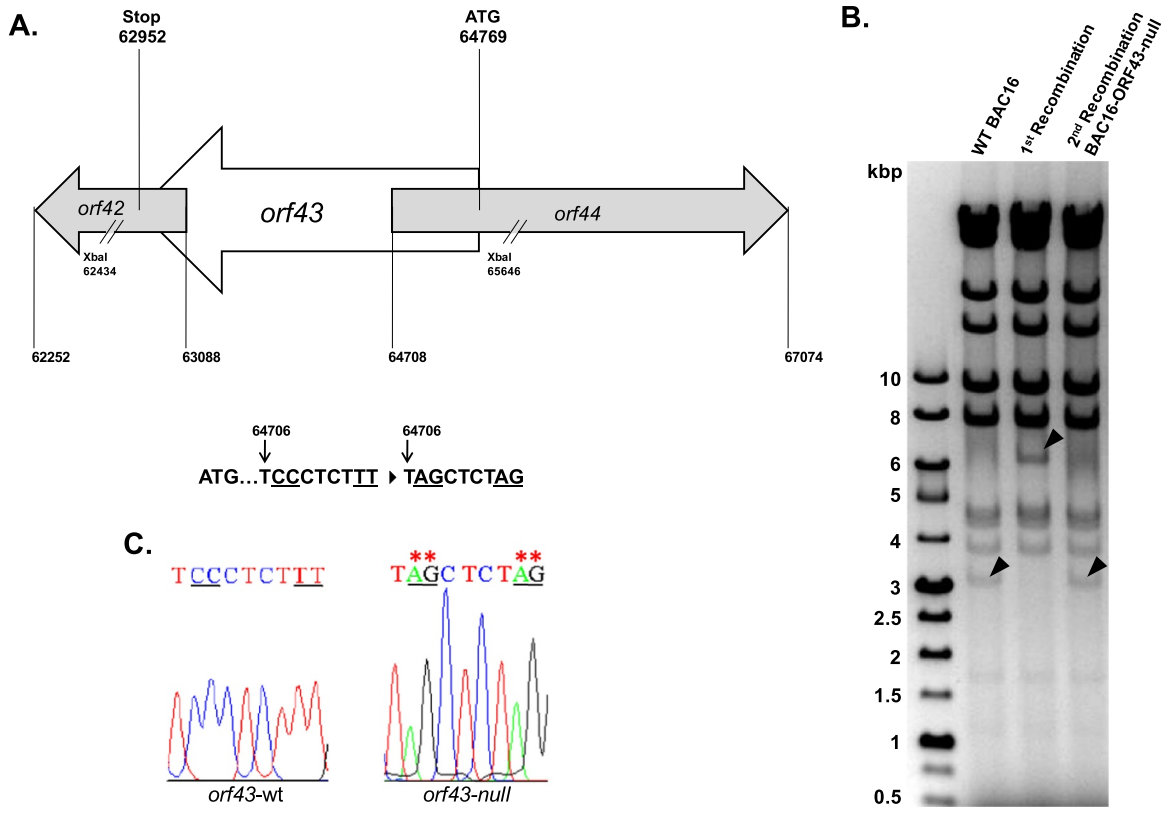

Fig. 4. *Construction and analysis of recombinant BAC16-ORF43-null virus.* Schematic illustration of wild-type (WT) KSHV genome encoding ORF43. The nucleotide positions (GenBank accession number GQ994935.1) are indicated below the diagram, as are the ORF43 initiation methionine (ATG) and the stop codons. Genomic positions of *Xba*I restriction sites are indicated. Mutations sites are shown below the WT genome (A). Agarose gel electrophoresis of WT BAC16, BAC16 after the first recombination (1st recombination), and the resulting recombinant BAC16-ORF43-null (2nd recombination). BAC DNA was digested with *Xba*I, resolved on a 0.4% agarose gel and stained with ethidium bromide. As predicted, the ORF43-null BAC16 mutant shared a similar restriction pattern with WT. Altered bands, resulting from insertion of a Kanamycin cassette after the 1st recombination, are indicated by arrows. Molecular weight markers (M) are shown on the left (B). Sequence analysis of the recombinant BAC16-ORF43-null (left - *orf43-WT,* right - *orf43-null*) (C).

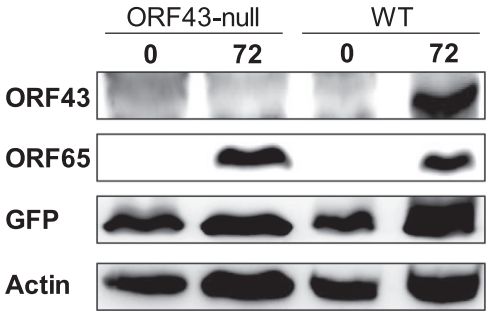

Fig. 5. *BAC16-ORF43-null-infected HEK-293T cells fail to express ORF43 upon lytic induction.* BAC16-ORF43-null and WT BAC16-infected HEK-293T cells were transduced with recombinant baculovirus that expresses RTA and treated with 1 mM sodium butyrate to induce lytic virus reactivation. 72-hr post induction cells were lysed and analyzed as described in Fig. 1.

proper portal structures enabling packaging of the mutated BAC16-ORF43-null DNA. Nevertheless, our analysis suggests that vast majority of the virions obtained contain mutant BAC16-ORF43-null genome. Furthermore, by using these sets of primers we amplified packaged DNase-resistant WT *orf43* which was concentrated from WT BAC16-infected cells, but failed to amplify DNase-resistant WT or mutated *orf43* in concentrated supernatants from BAC16-ORF43-null infected cells (Fig. 7B). These findings, along with the failure of BAC16-ORF43-null virions to produce GFP-positive cells upon their inoculation, indicate that ORF43-null recombinant virus fails to package genomic viral DNA.

2.4. KSHV-ORF43-null cannot produce C-capsids

Three types of capsids are generated during herpesvirus assembly. Two types, A and B, lack genomic viral DNA and are either empty or contain different amounts of residual scaffold protein, respectively, whereas the third type, the C-capsid, is occupied with genomic viral DNA. The portal ring is required for the production of C-capsids (Deng et al., 2008). To examine capsid production and to characterize the capsid types that are produced by BAC16-ORF43-null-infected cells, we employed transmission electron microscopy (TEM) on iSLK cells that were induced to undergo lytic induction for 72-hr. As shown in Fig. 8, unlike WT BAC16 which produced A, B and C capsids, BAC16-ORF43-null mutant did not produce C-type capsids. Quantitative analysis of 566 capsids from 10 WT BAC16-infected cells revealed 5%, 67% and 28% A, B and C-type capsids, respectively, whereas similar analysis of 149 capsids from 10 BAC16-ORF43-null-infected cells revealed 2.5% and 97.5% A and B-type capsids, respectively. This indicates that capsids are assembled in cells that are infected with BAC16-ORF43-null viruses, but the viral genomic DNA is not inserted into the capsids.

3. Discussion

Productive viral infection involves expression of gene products that are not always essential. However, this is not the case with regard to a set of herpesviral structural proteins that participate in capsid assembly and maturation and in packaging of genomic viral DNA. We anticipated that the KSHV ORF43 protein, which shares homology with portal proteins of other herpesviruses, is essential for the production of infectious progeny viruses. In the present study, we used the full-length

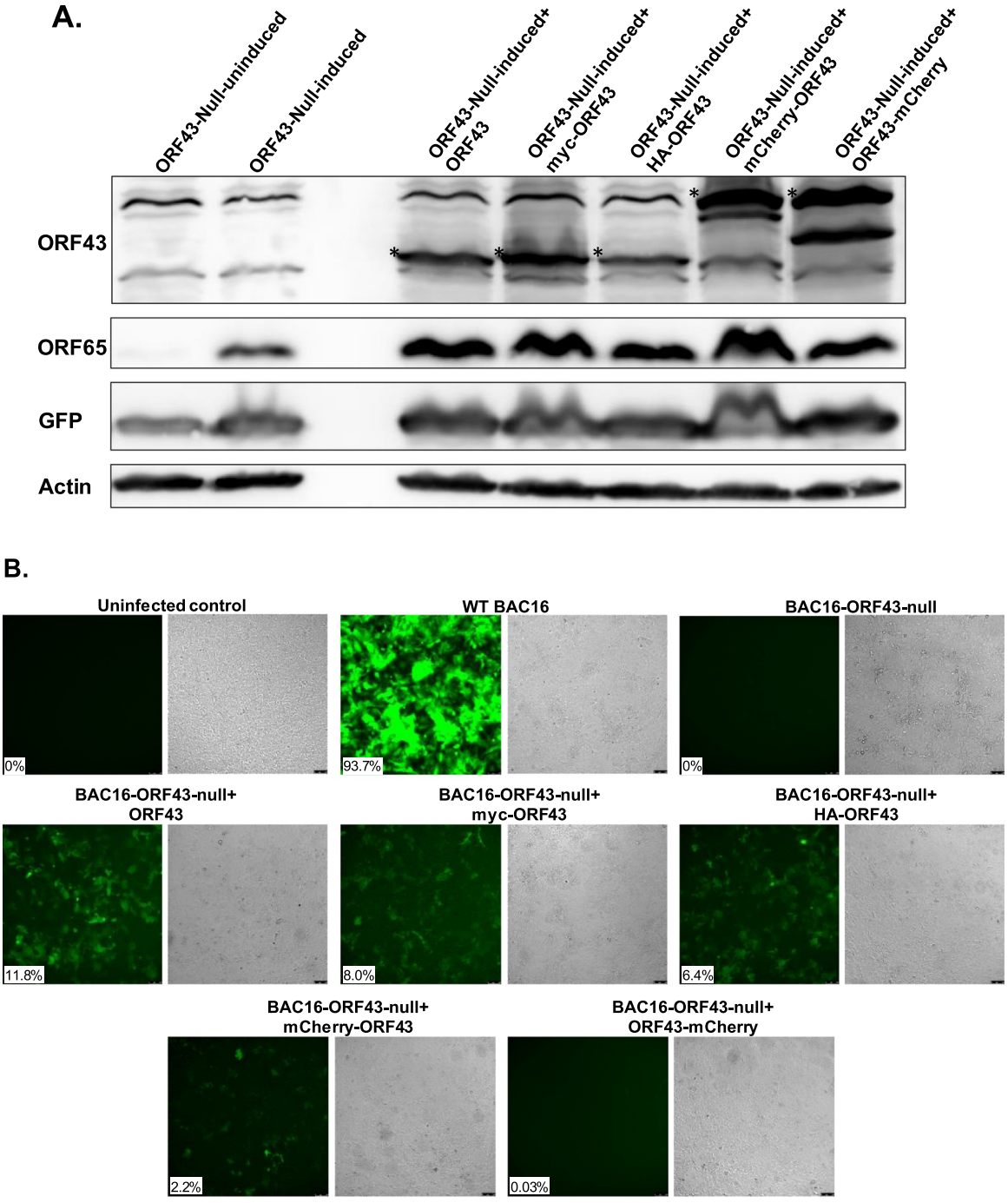

Fig. 6. *Ectopic expression of un-tagged and tagged ORF43 protein enables production of infectious virions.* BAC16-ORF43-null infected HEK-293T cells were transfected with the indicated expression plasmids (ORF43, myc-ORF43, HA-ORF43, mCherry-ORF43 and ORF43-mCherry). 24-hr post transfection cells were transduced with a recombinant baculovirus which expresses RTA and treated with 1 mM sodium butyrate to induce lytic replication. WB analysis with antibodies to ORF65 and ORF43 confirmed lytic induction and ectopic expression of ORF43, respectively (asterisks indicate ORF43). Uninduced and induced BAC16-ORF43-null infected cells were used as controls (A). Supernatants were collected 96-hr post induction, concentrated, and used to infect SLK cells. Infected cells were detected as GFP-positive. Images were captured 72-hr post infection and GFP was quantified with ImageJ software. % GFP-positive area, representing average of 7 images, is shown. Control uninfected, WT BAC16-infected and BAC16-ORF43-null infected cells are also shown. Scale bars 100 μM. Results shown represent one experiment representative of three providing similar results (B).

KSHV clone BAC16 to generate a recombinant virus that contains two stop mutations within the coding sequence of ORF43. This recombinant virus, termed BAC16-ORF43-null, established latent infection upon transfection of its DNA, and upon lytic induction, produced capsids that were similar in size to their WT counterparts. Yet, this mutant virus failed to package viral DNA and to produce infectious progeny virions and no C-type particles with electron-dense cores were observed by TEM analysis. Accordingly, our findings suggest that assembly of the KSHV capsids in cells may initiate and proceed in the absence of ORF43, though this protein is essential for the production of infectious viral particles. These findings are consistent with other herpesviruses, revealing that viral capsids can be assembled but infectious particles cannot be produced in the absence of full-length portal protein (Lamberti and Weller, 1996; Patel et al., 1996; Pavlova et al., 2013).

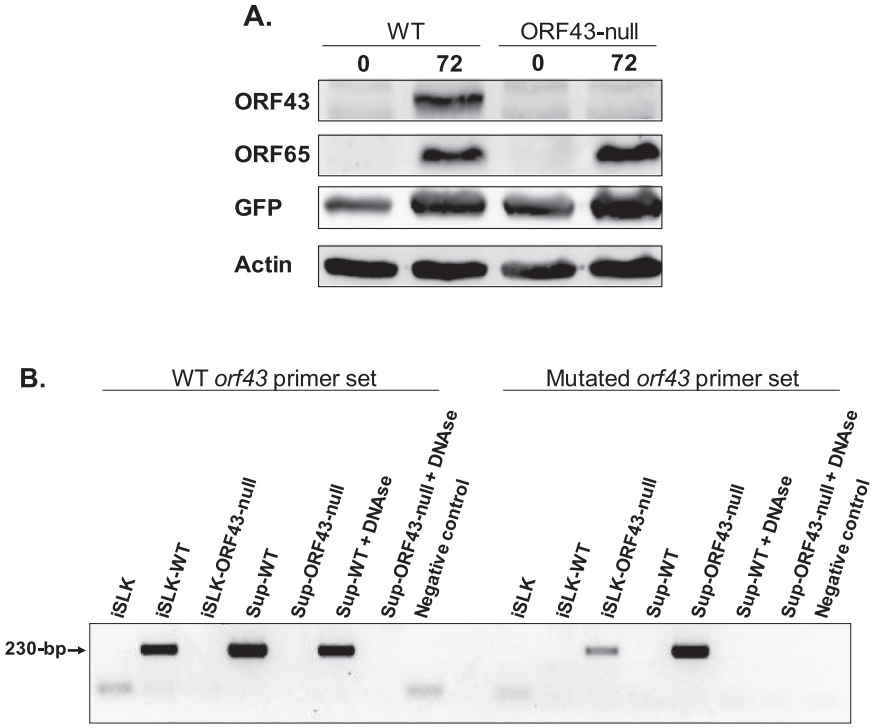

Fig. 7. *BAC16-ORF43-null-infected iSLK cells fail to express ORF43 and produce virions that lack genomic viral DNA.* iSLK cells were infected with virions from WT BAC16-infected HEK-293T cells and BAC16-ORF43-null-infected cells that ectopically expressed ORF43 resulting in persistent latent infection. These cells were induced to undergo lytic reavtivation by 1 μg/ml Doxycycline (Dox) and 1 mM sodium butyrate. Protein extracts were prepared and assayed for ORF65 and ORF43 expression (A). Supernatants (Sup) were collected 96-hr post induction and concentrates containing equal quantities of virions were either left untreated or treated with DNase to remove free DNA. Uninfected, WT BAC16 or BAC16-ORF43-null-infected iSLK cells ($3x10^4$ cells per reaction) were used as controls. Reaction mixtures containing DNase, but no template, were used as negative controls. PCR employed two sets of primers to selectively amplify WT or mutated *orf43*. 230-bp PCR products were obtained with WT and mutated primer sets employing WT-BAC16 and BAC16-ORF43-null-infected iSLK cells, respectively. PCR product was also obtained from untreated and DNase-treated supernatants from WT BAC16-infected cells using the WT *orf43* primer set. In contrast, PCR product was obtained from BAC16-ORF43-null untreated supernatants by using the mutated *orf43* primer set whereas no product was obtained upon DNase treatment of this supernatant, thus indicating lack of packaged genomic viral DNA in BAC16-ORF43-null virions.

Consistent with our results, previous *in vitro* studies demonstrated assembly of herpesviral capsids, including KSHV, in the absence of the portal protein (Motwani et al., 2017; Newcomb et al., 2005; Perkins et al., 2008; Tatman et al., 1994; Thomsen et al., 1994).

Ectopic expression of ORF43 enabled production of virions containing the mutated *orf43* viral genome, which in-turn could infect cells and establish latent infection. Accordingly, we conclude that the BAC16-ORF43-null virus does not contain mutations beyond those that we deliberately introduced. Yet, it was surprising to find that all the ectopically expressed ORF43 proteins rescued the BAC16-ORF43-null mutated phenotype, despite their altered subcellular distribution though at different efficiencies. This was most unexpected for mCherry and HA-tagged ORF43 proteins that were shown to be predominantly expressed in the cytoplasm. Because we were concerned about the development of revertant wild-type (WT) genomes, we developed a PCR assay which discriminates between WT and mutated *orf43* within the genomic viral DNA. Using this assay, we confirmed that iSLK cells that were infected with virions that were collected from BAC16-ORF43-null-infected cells upon lytic induction and ectopic expression of the different ORF43 proteins, contained mutated viral genomes. Yet, this assay cannot formally exclude the occurrence of rare recombination events producing wild type genomes that enable production of proper capsids which package mutated genomes. Accordingly, further studies are required to track the mechanism by which the different recombinant proteins rescued production of infectious viral particles.

Since capsid assembly takes place in the nucleus during late phases of lytic infection, ORF43 was expected to present late expression kinetics and to localize in this compartment during lytic replication. As predicted, using the antiserum we produced, we identified ORF43 as a late viral protein which is expressed in the nucleus during lytic reactivation. ORF43 expression kinetics and cell localization corresponded to that of the small capsid protein, ORF65. Similarly, ectopically expressed untagged and myc-tagged ORF43 proteins were predominantly localized in the nucleus, suggesting that nuclear localization of ORF43 does not require additional viral proteins. In contrast, HA and mCherry-tagged ORF43 were predominantly cytoplasmic, and large cytoplasmic aggregates were evident upon expression of HA-ORF43. Similar cytoplasmic-granular localization with Golgi enrichment has been previously described for ORF43 containing the His-myc tag at the carboxyl terminus (Sander et al., 2008). Of note, different bioinformatic tools failed to identify a nuclear localization signal in ORF43. Together, these results indicate that care should be taken with regard to ORF43 tagging since the tag, and even a small one, may affect protein solubility, cellular localization, and function.

Structural, as well as non-structural viral proteins can potentially serve as targets for therapeutic interventions. Indeed, specific thiourea compounds selectively target herpesviral portal proteins and inhibit virus propagation. Furthermore, selected mutations in the portal protein provide resistance to these compounds (Newcomb and Brown, 2002; van Zeijl et al., 2000; Visalli et al., 2003; Visalli and van Zeijl, 2003). The reagents generated in the present study are expected to enable further studies of ORF43. In addition, BAC16-ORF43-null virus may serve in the future as a platform to screen for specific ORF43 mutations that prevent proper capsid assembly or provide drug resistance to encapsidation-specific antiviral inhibitors.

4. Materials and methods

4.1. Plasmids

ORF43 expression plasmids containing different tags were generated (Table 1). DNA inserts were synthesized by PCR amplification using BAC16 DNA as template and appropriate primers (Sigma). DNA cloning employed digestion of inserts and vectors using restriction enzymes (New England Biolabs, Ipswich, MA) and ligation with T4 DNA ligase (Biogase Fast Ligation Kit, Bio-Lab). Ligation products were transformed into DH5α, grown on appropriate selection medium, and examined by colony PCR and restriction enzyme analysis of purified plasmid DNAs (AccuPrep Plasmid Mini-Extraction Kit, Bioneer). All cloned PCR products were verified by sequencing.

4.2. Cell culture and transfection

Human epithelial kidney HEK-293T cells, renal cell carcinoma SLK and iSLK cells (kindly provided by Don Ganem, Howard Hughes Medical Institute, UCSF, San Francisco, CA, and Rolf Renne, University

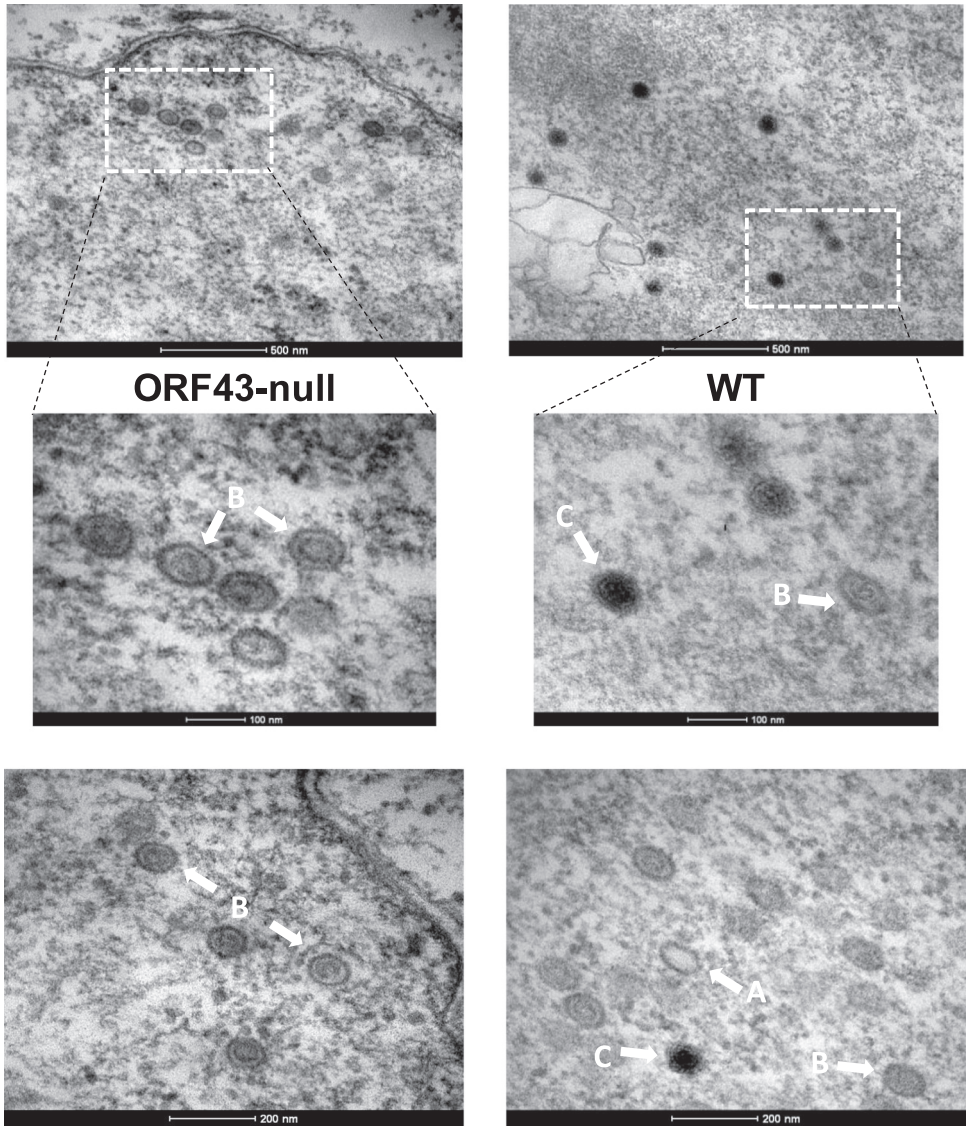

Fig. 8. *TEM microphotographs of WT BAC16 and BAC16-ORF43-null-infected cells.* iSLK cells infected with WT BAC16 or BAC16-ORF43-null were induced to undergo lytic infection by 1 μg/ml Doxycycline (Dox) and 1 mM sodium butyrate. Cells were harvested 72-hr post induction and examined by transmission electron microscopy.

Table 1
List of expression plasmids and primers used to obtain inserts.

Plasmid	Restriction Enzymes	Vector	Primers
mCherry- *orf*43	*Eco*RI-*Bam*HI	mCherry-C1	5'-TTTGAATTCTTTGAGGATGAACCCGGGGCT – 3' 5'-TTTGGATCCCTATGCACTTCCAGGACAAG – 3'
*orf*43-mCherry	*Nhe*I-*Xho*I	mCherry-N1	5'-TTTGCTAGCCCGATGTCATGTTGA – 3' 5'-TTTCTCGAGTGCACTTCCAGGACA – 3'
myc- *orf*43-Zeo	*Bam*HI-*Eco*RI	pcDNA3.1/Zeo	5'-TTTGGATCCGCCGCCATGGAGCAGAAACTCA TCTCTGAAGAGGATCTGTTGAGGATGAACCCGGGGCT – 3' 5'-TTTGAATTCCTATGCACTTCCAGGACAAG – 3'
pETMBPH-*orf*43C	*Bam*HI-*Eco*RI	pETMBPH	5'-TTTGGATCCGAGCTCCTCAACCTGCTCAT – 3' 5'-TTTGAATTCCTATGCACTTCCAGGACAAG – 3'
HA- *orf*43	*Nhe*I-*Eco*RI	pcDNA3.1/Zeo	5'-AAAGCTAGCACGATGGCTTACCCATACGA TGTTCCAGATTACGCACGTGGATCCTTGAGGATGAACCCGGGGCT – 3' 5'-TTTGAATTCCTATGCACTTCCAGGACAAG – 3'
*orf*43	*Bam*HI-*Eco*RI	pcDNA3.1/Zeo	5'-TTTGGATCCCCGATGTCATGTTGAGGATG – 3' 5'-TTTGAATTCCTATGCACTTCCAGGACAAG – 3'

of Florida, Gainesville, FL) (Myoung and Ganem, 2011; Sturzl et al., 2013) were grown in Dulbecco's modified Eagle's medium (DMEM) (Biological Industries, Israel) containing 50 IU/ml penicillin and 50 μg/ml streptomycin (Biological industries, Israel), and supplemented with 10% heat-inactivated fetal calf serum (FCS) (Biological Industries, Israel). iSLK cells were grown in the presence of 250 μg/ml G418 and 1 μg/ml Puromycin (A.G. Scientific Inc.) to maintain the Tet-on transactivator and the RTA expression cassette, respectively. The growth medium of BAC16-infected HEK-293T and iSLK cells was supplemented with 200 and 600 μg/ml hygromycin (MegaPharm, San Diego, CA), respectively, to maintain KSHV episomes. 0.5 μM Phosphonoacetic acid (PAA) (Sigma) was added to inhibit viral DNA replication. Transient transfections of plasmid DNA employed the calcium phosphate precipitation method.

4.3. Production of rabbit antibodies to ORF43

The ORF43 carboxyl terminal fragment (amino acids 306–605) was cloned into the pETMBPH expression plasmid. This plasmid was transformed into BL21-NT+ *E. coli* cells which are enriched for extra copies of tRNA genes that are rare in *E. coli* along with a chloramphenicol resistance gene. Plasmid transformed bacteria were grown on medium containing 34 μg/ml chloramphenicol and 15 μg/ml Kanamycin. To obtain sufficient amounts of purified protein, a single colony was inoculated in 1 ml LB broth medium (Sigma) containing antibiotics, and then this starter was seeded in LB and incubated overnight at 37 °C. The next day, the culture was diluted 1:40 in 12 liters of 2YT medium (16 gr/L Trypton; 10 gr/L Yeast extract; 5 gr/L NaCl) containing both antibiotics, and grown at 37 °C until reaching $OD_{600\,nm}$ of 0.3, then transferred to 18 °C until reaching $OD_{600\,nm}$ of 0.6. To induce protein expression, 0.1 mM Isopropyl β-D-1-thiogalactopyranoside (IPTG) was added and growth continued overnight. The protein was harvested by centrifugation of the bacterial culture at 3000 × g for 25 min at 4 °C, and frozen pellet was suspended in buffer A (25 mM Tris; 500 mM NaCl; 5% Glycerol pH 7.8) containing a cocktail of protease inhibitors (Complete EDTA-free protease inhibitor cocktail tablets without EDTA, Roche Diagnostic Mannheim, Germany) and 1 mM DTT. After grinding the bacteria with homogenizer, cells were lysed with a microfluidizer, 0.2 mM phenylmethylsulfonyl fluoride (PMSF) was added, and the lysates were centrifuged twice at 24,000 × g for 20 min at 4 °C. Pellet and supernatant were analyzed by SDS-PAGE which was stained with Coomassie Imperial Protein Stain solution (Thermo Scientific, Waltham, MA). While most of the ORF43 protein remained insoluble in the pellet, protein purification was continued from the supernatant fraction which was loaded on Nickel column (HisTrap™HP, GE Healthcare Life Sciences). Elution was carried by using AKTA purifier (GE Healthcare Life Sciences) with buffer A containing 1 mM DTT and increasing imidazole concentrations (25–125 mM), and fractions were analyzed by SDS-PAGE. Two fractions in which ORF43 was most abundant (from 100 to 115 mM imidazole solution) were concentrated in 10-kDa filter tube (Millipore™ Amicon Ultrocentrifugal Filter Units) resulting in 1.5 ml of protein at a concentration of 2.2 mg/ml. Of note, attempts to digest the recombinant protein with TEV were unsuccessful. The resulting MBP-6His-TEV-ORF43C protein was injected into two rabbits (Sigma, Israel), and sera were obtained and tested against the purified antigen.

4.4. Antibodies and western blot analysis

Cells were washed twice in cold phosphate-buffered saline (PBS), and suspended in radio-immunoprecipitation assay (RIPA) lysis buffer, or solubilization buffer (50 mM HEPES (pH 7.5), 150 mM NaCl, 1% Triton X-100, 10% glycerol, 1 mM EDTA (pH 8.0), 1 mM EGTA (pH 8.0), 1.5 mM $MgCl_2$), containing the protease inhibitors PMSF and a commercial cocktail (Complete, Roche Diagnostics). Cells in lysis buffer were incubated on ice for 20 min, and centrifuged at 13,300 × g for 15 min at 4 °C, to remove cell debris. Sodium-dodecyl sulfate (SDS) loading buffer was added, and the samples were boiled for 5 min. Protein lysates were resolved by SDS-PAGE and transferred to nitrocellulose membranes using Trans-blot Turbo RTA Midi Nitrocellulose Transfer Kit (Bio-Rad, Berkeley, CA). The protein content of the different samples was verified by Ponceau S staining. The membranes were blocked with 5% dry milk in Tris-buffered saline (TBS) and then incubated with rabbit anti-ORF43 or mouse antibody to GFP (Covance Research Products, Denver, CO), ORF45 (Zhu et al., 2005), ORF K8 (Wang et al., 2008) (a kind gift from Prof. Yan Yuan), ORF65 (Ye et al., 2011) (a kind gift from Shou Jiang Gao), or RTA (Ueda et al., 2002) (kindly provided by Keiji Ueda). Immunoreactive bands were detected by anti-mouse or anti-rabbit antibodies conjugated to horseradish peroxidase (Jackson ImmunoResearch Laboratories, Inc., West Grove, PA). The bands were visualized with Clarity™ Westen ECL substrate (Bio-Rad).

4.5. Fluorescence and immunofluorescence microscopy

Cells were seeded on coverslips in a 24-well plate. After 24-h, transfection was performed as described above or cells were treated to induce lytic reactivation. Cells were washed several times with PBS (Biological Industries, Israel) 24–72-h post transfection or reactivation, and fixed in 4% formaldehyde in PBS for 20 min at room temperature. After fixation, cells were washed twice with PBS, permeabilized and blocked in PBS with 0.2% Triton X-100% and 1% BSA. Slides were incubated with primary antibody (anti-ORF43, anti-ORF65, anti HA (HA1.1) (Covance Research Products, Denver, CO) or anti-myc (myc-Tag 9B11) (Cell Signaling Technology, Boston, MA)) at 4 °C overnight, followed by incubation with secondary conjugated antibody (Rhodamine, Cy3 or Alexa 647, Jackson ImmunoResearch Laboratories, Inc., West Grove, PA) for 1-h at room temperature. To stain the nuclei, cells were incubated for 30 min with 0.05 μg/ml Hoechst dye (Sigma) in PBS. The slides were mounted with antifading medium (1% *n*-Propyl gallate, 90% Glycerol in PBS). Cells were examined and photographed under a confocal laser-scanning microscope (Leica SP8 Confocal Live Microscope).

4.6. Construction of recombinant BAC16-ORF43-null clone

Recombinant full-length KSHV BAC16 which constitutively expresses GFP under the control of the cellular elongation factor 1-alpha (EF-1α) was previously described and obtained as a kind gift from Prof. Jae Jung (Brulois et al., 2012). *Escherichia coli* GS1783 bacteria, encoding inducible Red recombination enzymes and I-SceI endonuclease, were used to construct the recombinant virus with a two-step recombination protocol (Bergson et al., 2016; Tischer et al., 2006). To construct a recombinant KSHV BAC16 clone which contains two stop codons in the *orf43* gene sequence, we generated a fragment containing the mutations by using pEGFP-C2 plasmid (Clontech) as a template for the kanamycin resistance gene. The primers used were

5`-CCCGGGGCTGGGCTCGTCCATATCAGTGCACCCTTCCGAGCTGTC CATC**TAG**C TC**TAG**GAGATCCTGCAAGGCAAGTATTAGGGATAACAGGG TAATAGGTGGCACTTTTCGGGGAAA-3` and 5`- CAGTGTAGAGTCTGAC CTCTGACATAAGAATACTTG CCTTGCAGGATCTC**CTA**GAG**CTA**GATGG ACAGCTCGGAAGGGTTTATTGCCGTCATAGCGCGG-3`. Stop codons are bolded and mutated nucleotides are underlined. Primers also contained a I-SceI recognition site, and 71-nt upstream and downstream of the mutations sites. The resulting Bacmid was confirmed by *Xba*I restriction enzyme digestion. The inserted mutated DNA fragment was sequenced to confirm the presence of the desired mutations and junction sequences at the insertion site. BAC DNA was purified using a large construct kit (Qiagen).

4.7. Transfection of KSHV BAC16 and BAC16-ORF43-null DNA and virus reconstitution

BAC16 and BAC16-ORF43-null reconstitution was carried as previously described (Bergson et al., 2016; Gelgor et al., 2015). Briefly, BAC DNA was transfected into HEK-293T cells using the Lipofectamine 2000 transfection reagent (Life Technologies, Invitrogen), and transfected cells were selected with 200 μg/ml hygromycin B (A. G. Scientific Inc.). Plasmids expressing un-tagged or tagged ORF43 protein were transfected into HEK-293T containing the Bac16-ORF43-null genome. Lytic reactivation was induced 24-hr post transfection with recombinant baculovirus that constitutively expresses RTA (BacK50) (kindly provided by Prof. David Lukac) (Lukac et al., 2001) and 1 mM sodium butyrate. Supernatants containing virions were collected 96-hr later, and cleared of cells and debris by centrifugation (700 × *g* for 10 min at 4°C) and filtration (0.45-μm cellulose acetate filters; Corning). iSLK cells were infected in the presence of 8 μg/ml polybrene by spinoculation (centrifugation at 1500 X g at 25°C for 60 min), which was followed by 1-hr incubation at 37°C, before changing the supernatant to fresh medium containing 5% FCS. Infected cells were selected in medium containing 600 μg/ml hygromycin B. KSHV-infected iSLK cells were treated with 1 μg/ml doxycycline and 1 mM sodium butyrate (Sigma), in the absence of hygromycin, puromycin, and G418, to induce RTA transgene expression and lytic cycle reactivation.

4.8. Distinction between WT and BAC16-ORF43-null genomes by PCR

To ensure that cells were infected with a mutated BAC16-ORF43-null genome, two sets of PCR primers were employed to selectively amplify WT or mutated *orf43*. DNA was amplified with 2xPCRBIO HS Taq Mix Red (PCR Biosystems) which allows direct amplification of unprocessed cell samples by using 5'-TCCTGCAGTCCCCGTTATTAC-3' forward primer together with 5'-TTGCAGGATCTCAAAGAGGG-3' or 5'-TTGCAGGATCTCCTAGAGCT-3' reverse primers, which amplify WT or mutated *orf43*, respectively, providing a product of 230-bp. $3x10^4$ cells per reaction were used for PCR amplification of cellular DNA template. iSLK cells harboring WT or ORF43-null virus were induced to undergo lytic reactivation using 1 μg/ml doxycycline and 1 mM sodium butyrate. Supernatants containing virions were collected 96-h post-induction, and cleared of cells and debris by centrifugation and filtration. Supernatants were then centrifuged (40,000 × *g* for 2-h at 4 °C) and the pellets were suspended in PBS and either left untreated or treated twice for 40 min at 37 °C with 10 units DNase (A&A Biothecnology, Poland) followed by DNase inactivation at 75 °C for 10 min. This procedure enabled degradation of free DNA whereas packaged virion DNA was protected by the capsid and could serve as PCR template. Of note, the later PCR assays employed similar quantities of viral particles as determined by WB with ORF65 antibodies that enable detection and quantification of virions.

4.9. Transmission electron microscopy (TEM)

Cells were seeded in 10 mm plates and a lytic cycle was induced 24-h later. 72-h post induction, cells were washed and fixed in para-formaldehyde and glutaraldehyde for 2-h at room temperature and then left at 4 °C for 72-h. Cells were then washed with 0.1 M sodium cacodylate buffer, harvested and suspended in 3.5 gr/ml warm agarose (Noble agar, Sigma) which was immediately cooled. Embedded cells were stained for 1-h with 1% osmium tetraoxide (OsO_4) (1% OsO_4 in 0.1 M sodium cacodylate buffer, 5 mM $CaCl_2$, 0.5% Potassium dichromate ($K_2Cr_2O_7$), 0.5% Potassium hexacyonaferrate ($K_4[Fe(CN)_6]$)), washed 3 times with the cacodylate buffer and then stained with 2% Uranyl acetate for 1-h. Embedded cells were dehydrated with increasing ethanol concentrations, and then with propylene oxide. The samples were then treated in increasing concentrations of Epon in propylene oxide until overnight embedding in 100% Epon and curing in 60 °C for 3 days. Thin sections were collected on copper grids and stained with Lead citrate. Cells were visualized with FEI Tecnai G^2 120 kV transmission electron microscope.

Acknowledgements

We thank Dr. Julia Guez-Haddad for her valuable advice and help in bacterial expression and purification of ORF43 protein, Dr. Avi Jacobs and Dr. Irit Shoval for their assistance with confocal microscopy, Dr. Ayelet Atkins from the BIU TEM Unit, and Dr. Ilana Loinger for her advice on PCR settings. We also thank Anastasia Gelgor for her constructive advices and help. We gratefully acknowledge Prof. Jae Jung, Don Ganem, Shou Jiang Gao, Yan Yuan, Keiji Ueda and David Lukac for gifts of reagents. This work was supported by a grant from the Israel Science Foundation (Grant no. 1365/15).

References

Baines, J.D., 2011. Herpes simplex virus capsid assembly and DNA packaging: a present and future antiviral drug target. Trends Microbiol 19, 606–613.
Bergson, S., Itzhak, I., Wasserman, T., Gelgor, A., Kalt, I., Sarid, R., 2016. The Kaposi's-sarcoma-associated herpesvirus orf35 gene product is required for efficient lytic virus reactivation. Virology 499, 91–98.
Bergson, S., Kalt, I., Itzhak, I., Brulois, K.F., Jung, J.U., Sarid, R., 2014. Fluorescent tagging and cellular distribution of the Kaposi's sarcoma-associated herpesvirus ORF45 tegument protein. J. Virol. 88, 12839–12852.
Brown, J.C., Newcomb, W.W., 2011. Herpesvirus capsid assembly: insights from structural analysis. Curr. Opin. Virol. 1, 142–149.
Brulois, K.F., Chang, H., Lee, A.S., Ensser, A., Wong, L.Y., Toth, Z., Lee, S.H., Lee, H.R., Myoung, J., Ganem, D., Oh, T.K., Kim, J.F., Gao, S.J., Jung, J.U., 2012. Construction and manipulation of a new Kaposi's sarcoma-associated herpesvirus bacterial artificial chromosome clone. J. Virol. 86, 9708–9720.
Cardone, G., Heymann, J.B., Cheng, N., Trus, B.L., Steven, A.C., 2012. Procapsid assembly, maturation, nuclear exit: dynamic steps in the production of infectious herpesvirions. Adv. Exp. Med Biol. 726, 423–439.
Cardone, G., Winkler, D.C., Trus, B.L., Cheng, N., Heuser, J.E., Newcomb, W.W., Brown, J.C., Steven, A.C., 2007. Visualization of the herpes simplex virus portal in situ by cryo-electron tomography. Virology 361, 426–434.
Chang, J.T., Schmid, M.F., Rixon, F.J., Chiu, W., 2007. Electron cryotomography reveals the portal in the herpesvirus capsid. J. Virol. 81, 2065–2068.
Chang, Y., Cesarman, E., Pessin, M.S., Lee, F., Culpepper, J., Knowles, D.M., Moore, P.S., 1994. Identification of herpesvirus-like DNA sequences in AIDS-associated Kaposi's sarcoma. Science 266, 1865–1869.
Deng, B., O'Connor, C.M., Kedes, D.H., Zhou, Z.H., 2007. Direct visualization of the putative portal in the Kaposi's sarcoma-associated herpesvirus capsid by cryoelectron tomography. J. Virol. 81, 3640–3644.
Deng, B., O'Connor, C.M., Kedes, D.H., Zhou, Z.H., 2008. Cryo-electron tomography of Kaposi's sarcoma-associated herpesvirus capsids reveals dynamic scaffolding structures essential to capsid assembly and maturation. J. Struct. Biol. 161, 419–427.
Dittmer, A., Bogner, E., 2006. Specific short hairpin RNA-mediated inhibition of viral DNA packaging of human cytomegalovirus. FEBS Lett. 580, 6132–6138.
Dittmer, D.P., Damania, B., 2013. Kaposi sarcoma associated herpesvirus pathogenesis (KSHV)–an update. Curr. Opin. Virol. 3, 238–244.
Gelgor, A., Kalt, I., Bergson, S., Brulois, K.F., Jung, J.U., Sarid, R., 2015. Viral Bcl-2 Encoded by the Kaposi's Sarcoma-Associated Herpesvirus Is Vital for Virus Reactivation. J. Virol. 89, 5298–5307.
Goncalves, P.H., Ziegelbauer, J., Uldrick, T.S., Yarchoan, R., 2017. Kaposi sarcoma herpesvirus-associated cancers and related diseases. Curr. Opin. HIV AIDS 12, 47–56.
Gramolelli, S., Schulz, T.F., 2015. The role of Kaposi sarcoma-associated herpesvirus in the pathogenesis of Kaposi sarcoma. J. Pathol. 235, 368–380.
Heming, J.D., Conway, J.F., Homa, F.L., 2017. Herpesvirus capsid assembly and DNA packaging. Adv. Anat. Embryol. Cell Biol. 223, 119–142.
Holzenburg, A., Dittmer, A., Bogner, E., 2009. Assembly of monomeric human cytomegalovirus pUL104 into portal structures. J. Gen. Virol. 90, 2381–2385.
Kalt, I., Masa, S.R., Sarid, R., 2009. Linking the Kaposi's sarcoma-associated herpesvirus (KSHV/HHV-8) to human malignancies. Methods Mol. Biol. 471, 387–407.
Kornfeind, E.M., Visalli, R.J., 2018. Human herpesvirus portal proteins: structure, function, and antiviral prospects. Rev. Med Virol. 28, e1972.
Lamberti, C., Weller, S.K., 1996. The herpes simplex virus type 1 UL6 protein is essential for cleavage and packaging but not for genomic inversion. Virology 226, 403–407.
Lukac, D.M., Garibyan, L., Kirshner, J.R., Palmeri, D., Ganem, D., 2001. DNA binding by Kaposi's sarcoma-associated herpesvirus lytic switch protein is necessary for transcriptional activation of two viral delayed early promoters. J. Virol. 75, 6786–6799.
McElwee, M., Vijayakrishnan, S., Rixon, F., Bhella, D., 2018. Structure of the herpes simplex virus portal-vertex. PLoS Biol. 16, e2006191.
Mesri, E.A., Cesarman, E., Boshoff, C., 2010. Kaposi's sarcoma and its associated herpesvirus. Nat. Rev. Cancer 10, 707–719.
Motwani, T., Lokareddy, R.K., Dunbar, C.A., Cortines, J.R., Jarrold, M.F., Cingolani, G., Teschke, C.M., 2017. A viral scaffolding protein triggers portal ring oligomerization and incorporation during procapsid assembly. Sci. Adv. 3, e1700423.

Myoung, J., Ganem, D., 2011. Generation of a doxycycline-inducible KSHV producer cell line of endothelial origin: maintenance of tight latency with efficient reactivation upon induction. J. Virol. Methods 174, 12–21.
Nealon, K., Newcomb, W.W., Pray, T.R., Craik, C.S., Brown, J.C., Kedes, D.H., 2001. Lytic replication of Kaposi's sarcoma-associated herpesvirus results in the formation of multiple capsid species: isolation and molecular characterization of A, B, and C capsids from a gammaherpesvirus. J. Virol. 75, 2866–2878.
Newcomb, W.W., Brown, J.C., 2002. Inhibition of herpes simplex virus replication by WAY-150138: assembly of capsids depleted of the portal and terminase proteins involved in DNA encapsidation. J. Virol. 76, 10084–10088.
Newcomb, W.W., Homa, F.L., Brown, J.C., 2005. Involvement of the portal at an early step in herpes simplex virus capsid assembly. J. Virol. 79, 10540–10546.
Newcomb, W.W., Juhas, R.M., Thomsen, D.R., Homa, F.L., Burch, A.D., Weller, S.K., Brown, J.C., 2001. The UL6 gene product forms the portal for entry of DNA into the herpes simplex virus capsid. J. Virol. 75, 10923–10932.
Newcomb, W.W., Thomsen, D.R., Homa, F.L., Brown, J.C., 2003. Assembly of the herpes simplex virus capsid: identification of soluble scaffold-portal complexes and their role in formation of portal-containing capsids. J. Virol. 77, 9862–9871.
Patel, A.H., Rixon, F.J., Cunningham, C., Davison, A.J., 1996. Isolation and characterization of herpes simplex virus type 1 mutants defective in the UL6 gene. Virology 217, 111–123.
Pavlova, S., Feederle, R., Gartner, K., Fuchs, W., Granzow, H., Delecluse, H.J., 2013. An Epstein-Barr virus mutant produces immunogenic defective particles devoid of viral DNA. J. Virol. 87, 2011–2022.
Perkins, E.M., Anacker, D., Davis, A., Sankar, V., Ambinder, R.F., Desai, P., 2008. Small capsid protein pORF65 is essential for assembly of Kaposi's sarcoma-associated herpesvirus capsids. J. Virol. 82, 7201–7211.
Sander, G., Konrad, A., Thurau, M., Wies, E., Leubert, R., Kremmer, E., Dinkel, H., Schulz, T., Neipel, F., Sturzl, M., 2008. Intracellular localization map of human herpesvirus 8 proteins. J. Virol. 82, 1908–1922.
Sturzl, M., Gaus, D., Dirks, W.G., Ganem, D., Jochmann, R., 2013. Kaposi's sarcoma-derived cell line SLK is not of endothelial origin, but is a contaminant from a known renal carcinoma cell line. Int J. Cancer 132, 1954–1958.
Tandon, R., Mocarski, E.S., Conway, J.F., 2015. The A, B, Cs of herpesvirus capsids. Viruses 7, 899–914.
Tatman, J.D., Preston, V.G., Nicholson, P., Elliott, R.M., Rixon, F.J., 1994. Assembly of herpes simplex virus type 1 capsids using a panel of recombinant baculoviruses. J. Gen. Virol. 75 (Pt 5), 1101–1113.
Thomsen, D.R., Roof, L.L., Homa, F.L., 1994. Assembly of herpes simplex virus (HSV) intermediate capsids in insect cells infected with recombinant baculoviruses expressing HSV capsid proteins. J. Virol. 68, 2442–2457.
Tischer, B.K., von Einem, J., Kaufer, B., Osterrieder, N., 2006. Two-step red-mediated recombination for versatile high-efficiency markerless DNA manipulation in Escherichia coli. Biotechniques 40, 191–197.
Trus, B.L., Cheng, N., Newcomb, W.W., Homa, F.L., Brown, J.C., Steven, A.C., 2004. Structure and polymorphism of the UL6 portal protein of herpes simplex virus type 1. J. Virol. 78, 12668–12671.
Trus, B.L., Heymann, J.B., Nealon, K., Cheng, N., Newcomb, W.W., Brown, J.C., Kedes, D.H., Steven, A.C., 2001. Capsid structure of Kaposi's sarcoma-associated herpesvirus, a gammaherpesvirus, compared to those of an alphaherpesvirus, herpes simplex virus type 1, and a betaherpesvirus, cytomegalovirus. J. Virol. 75, 2879–2890.
Ueda, K., Ishikawa, K., Nishimura, K., Sakakibara, S., Do, E., Yamanishi, K., 2002. Kaposi's sarcoma-associated herpesvirus (human herpesvirus 8) replication and transcription factor activates the K9 (vIRF) gene through two distinct cis elements by a non-DNA-binding mechanism. J. Virol. 76, 12044–12054.
van Zeijl, M., Fairhurst, J., Jones, T.R., Vernon, S.K., Morin, J., LaRocque, J., Feld, B., O'Hara, B., Bloom, J.D., Johann, S.V., 2000. Novel class of thiourea compounds that inhibit herpes simplex virus type 1 DNA cleavage and encapsidation: resistance maps to the UL6 gene. J. Virol. 74, 9054–9061.
Visalli, M.A., House, B.L., Selariu, A., Zhu, H., Visalli, R.J., 2014. The varicella-zoster virus portal protein is essential for cleavage and packaging of viral DNA. J. Virol. 88, 7973–7986.
Visalli, R.J., Fairhurst, J., Srinivas, S., Hu, W., Feld, B., DiGrandi, M., Curran, K., Ross, A., Bloom, J.D., van Zeijl, M., Jones, T.R., O'Connell, J., Cohen, J.I., 2003. Identification of small molecule compounds that selectively inhibit varicella-zoster virus replication. J. Virol. 77, 2349–2358.
Visalli, R.J., Howard, A.J., 2014. Non-axial view of the varicella-zoster virus portal protein reveals conserved crown, wing and clip architecture. Intervirology 57, 121–125.
Visalli, R.J., van Zeijl, M., 2003. DNA encapsidation as a target for anti-herpesvirus drug therapy. Antivir. Res 59, 73–87.
Wang, Y., Li, H., Tang, Q., Maul, G.G., Yuan, Y., 2008. Kaposi's sarcoma-associated herpesvirus ori-Lyt-dependent DNA replication: involvement of host cellular factors. J. Virol. 82, 2867–2882.
Wu, L., Lo, P., Yu, X., Stoops, J.K., Forghani, B., Zhou, Z.H., 2000. Three-dimensional structure of the human herpesvirus 8 capsid. J. Virol. 74, 9646–9654.
Ye, F., Zhou, F., Bedolla, R.G., Jones, T., Lei, X., Kang, T., Guadalupe, M., Gao, S.J., 2011. Reactive oxygen species hydrogen peroxide mediates Kaposi's sarcoma-associated herpesvirus reactivation from latency. PLoS Pathog. 7, e1002054.
Zhu, F.X., Chong, J.M., Wu, L., Yuan, Y., 2005. Virion proteins of Kaposi's sarcoma-associated herpesvirus. J. Virol. 79, 800–811.